ELSEVIER

Journal of Photochemistry and Photobiology A: Chemistry 101 (1996) 151–161

Journal of PHOTOCHEMISTRY AND PHOTOBIOLOGY A: CHEMISTRY

# Ground and excited singlet states of 2-vinylnaphthalene, ethyl-2-naphthylacrylate and *N,N*-dimethyl-2-naphthylacrylamide in solution

Frederick D. Lewis *, John M. Denari

*Department of Chemistry, Northwestern University, Evanston, Illinois 60208, USA*

Received 31 January 1996; accepted 17 April 1996

**Abstract**

The molecular conformation, spectroscopy and photochemical behavior of 2-vinylnaphthalene and its acrylate and acrylamide analogs were investigated. All three molecules exist as mixtures of syn and anti conformers. Ground state conformer populations were studied by nuclear Overhauser effect (NOE) spectroscopy and MM2 calculations. The electronic structure and spectra of the syn and anti conformers were investigated by INDO/S-SCF-CI calculations and were found to be very similar. Dual exponential fluorescence decay is observed for these molecules and is attributed to fluorescence from both the syn and anti conformers. The absence of a wavelength dependence for the fluorescence excitation and emission spectra provides experimental evidence that the syn and anti conformers have similar spectra. Photoisomerization of the acrylate and acrylamide occurs via a triplet state mechanism. Quenching of the acrylate singlet states by amines is more rapid for the syn relative to the anti conformer. Quenching by secondary and tertiary amines results in the regioselective formation of N–H and $\alpha$-C–H adducts respectively. The quantum yields of photoisomerization and photoaddition were determined for a mixture of the conformers, but were not separated into values for the individual conformers. The spectroscopy and photochemistry of ethyl-1-naphthylacrylate, which exists as a single conformer, were also investigated.

*Keywords:* Conformational isomers; Fluroescence; Photoaddition of amines; Photoisomerization

## 1. Introduction

A significant number of 1,2-diarylethenes have been observed to exhibit fluorescence from two singlet state conformational isomers [1]. The prototype for such behavior is *trans*-1-(2-naphthyl)-2-phenylethene which exists in the ground state as an equilibrium mixture of syn (s-cis) and anti (s-trans) conformers s-**1** and a-**1**. The absorption and fluorescence spectra of s-**1** and a-**1** overlap, but are sufficiently different to permit decomposition into pure component spectra [2]. The differences in the spectra, singlet lifetimes and fluorescence rate constants for s-**1** and a-**1** have been attributed to differences in the excited state electronic configuration [3]. Excited state conformers can also differ in their rates of unimolecular isomerization [2,4] and bimolecular reactions, such as electron transfer quenching by tertiary amines [5].

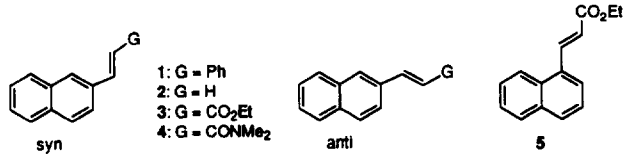


Arylethenes can also exist as mixtures of conformers. Indeed, the initial proposal by Cherkasov [6] of distinct fluorescence from two conformers was based on observations of the temperature-dependent fluorescence of 2-vinylanthracene. 2-Vinylnaphthalene should also exist as a mixture of syn and anti conformers s-**2** and a-**2**; however, Gustav and Schreiber [7] predicted that there should be little difference in their spectroscopic properties. Recently, Pfanstiel and Pratt [8] reported that the fluorescence of **2** in a supersonic jet displays two closely spaced origins attributed to s-**2** and a-**2**.

β-Arylacrylates can also exist as mixtures of conformers; however, there have been no reports of their conformer-dependent photochemical behavior. In this paper, we report the results of an investigation of the solution phase molecular structure, electronic spectra and photochemical behavior of

* Corresponding author.


*PII* S1010-6030(96)04387-0

**2** and its ester and amide derivatives **3** and **4**. For comparison, the behavior of the 1-naphthylacrylate **5**, which exists as a single conformer, has also been investigated. The fluorescence and photoisomerization of **3** and **5** have been investigated previously by Tanaka et al. [9]; however, the possible involvement of two ground state conformers was not considered. We find that **2–4** exist as mixtures of ground state conformers which have different singlet lifetimes, but virtually identical electronic spectra. The unimolecular photoisomerization and bimolecular reactions of **3–5** with amines have also been investigated.

## 2. Experimental details

### 2.1. General methods

IR spectra of 0.02 M solutions in $CHCl_3$ were recorded in 0.1 mm path length NaCl cells using a Mattson Fourier transform IR (FTIR) spectrophotometer. $^1H$ and $^{13}C$ nuclear magnetic resonance (NMR) spectra were recorded on a Varian-Gemini 300 spectrometer using $CDCl_3$ as solvent with tetramethylsilane as internal standard. Nuclear Overhauser effect (NOE) spectra were measured using a Bruker AMX-600 or Varian XLA 400. High-resolution mass spectra were recorded using a Hewlett Packard 5985 GC/VG analytical 70-250SE MS apparatus with an ionizing voltage of 70 V. Melting points (m.p.) were measured on a Fisher-Johns melting point apparatus and are uncorrected. UV absorption spectra were recorded on a Hewlett-Packard 8452A diode array spectrophotometer. Reduction potentials were measured on a BAS CV27 voltammeter in acetonitrile using 0.1 M $Et_4NBF_4$ as electrolyte and ferrocene as reference (half-wave potential, 0.680 V). Ag/AgI was used as reference electrode with glassy carbon as working electrode. The auxiliary electrode was a platinum wire of 1.6 mm in diameter.

Steady state fluorescence spectra were recorded on a Perkin–Elmer MPF-44A or a Spex Fluoromax spectrometer. All solutions ($(1–5)\times10^{-5}$ M) for fluorescence studies were contained in 1 cm path length quartz cuvettes sealed with septa and purged with nitrogen. Low-temperature fluorescence studies were carried out in an Oxford Instruments DN1704 variable temperature liquid nitrogen cryostat equipped with an ITC4 temperature controller. Fluorescence quantum yields were determined relative to pyrene at 296 nm ($\Phi_f=0.32$ [10]) for solutions of matched absorbance (approximately 0.1 OD). Fluorescence decays were obtained on a Photon Technology International LS-1 single-photon counting apparatus with a gated hydrogen arc lamp (time resolution, approximately 0.2 ns) using a scatter solution to approximate the lamp decay. Decays were analyzed using deconvolution and single- or multi-exponential least-squares fitting as described by James et al. [11]. The goodness of the fit was judged by the reduced $\chi^2$ value (less than 1.2 in all cases), the randomness of the residuals and the autocorrelation function.

Quantum yields of photoisomerization and amine addition were measured on an optical bench equipped with a 200 W high-pressure Oriel mercury–xenon lamp and a Bausch & Lomb high-intensity monochromator. Solutions contained in quartz cuvettes fitted with septa were purged with nitrogen and stirred during irradiation. Irradiated solutions were analyzed for product formation at less than 5% conversion using a Hewlett-Packard 5890 gas chromatograph equipped with a fused silica column coated with polymethyldisiloxane and a flame ionization detector. Light intensities were determined using the photoisomerization of *trans*-stilbene as actinometer [12].

Preparative irradiations were conducted in a Rayonet photochemical reactor equipped with 300 nm lamps. Hexane solutions containing 0.01 M **3–5** and 0.1 M amine were placed in Corning Glass 10 mm (outside diameter) Pyrex test tubes sealed with septa and purged with nitrogen. The reactions were monitored by gas chromatography (GC) analysis and terminated after approximately 80% conversion of the starting material. Yields of product formation were determined by GC analysis. Products were isolated by thick-layer chromatography (eluent, 10% MeOH in chloroform).

INDO/S-SCF-CI (ZINDO) calculations were performed using the method developed by Zerner and coworkers [13] as implemented by Lewis et al. [14] and performed on a Stellar mini supercomputer. Minimum energy conformations were calculated using a Macintosh IIsi computer with an MM2 type force field as supplied in the CHEM 3D software package [15].

### 2.2. Materials

All solvents used were of spectral grade. Hexane (Aldrich), anhydrous diethyl ether (Fisher) and acetonitrile (Aldrich) were used without further purification. Diethylamine (Fisher) and triethylamine (Fisher) were distilled under nitrogen prior to use. Trimethylamine (Fluka) was used without further purification. 2-Vinylnaphthalene (Aldrich) was sublimated twice prior to use.

#### 2.2.1. *trans*-Ethyl-2-naphthylacrylate (3)

Reaction of 1.0 g of 2-naphthaldehyde (Aldrich) with 6.10 g of (carboethoxymethyl)triphenylphosphonium bromide (Aldrich) by the method of Sugasawa and Matsuo [16], followed by column chromatography (eluent, 50% chloroform in hexane), afforded a mixture of cis and trans isomers. The mixture was dissolved in benzene and photoisomerized in the presence of iodine to provide **3** in 73% yield as a crystalline solid (m.p., 63–65 °C) (the methyl ester has been characterized previously [17]). $^1H$ NMR $\delta$: 7.94–7.50 (m, 7H), 7.86 (d, $J=15.9$ Hz, 1H), 6.56 (d, $J=15.9$ Hz, 1H), 4.30 (q, $J=7.1$ Hz, 2H), 1.37 (t, $J=7.1$ Hz, 3H). $^{13}C$ NMR (decoupled) $\delta$: 167.2, 144.7, 134.2, 133.3, 132.0, 130.0, 128.7, 128.6, 127.8, 127.3, 126.8, 123.5, 118.4, 60.6, 14.4.

High-resolution mass spectrometry (HRMS) $m/z$: 226.0994 (calculated); 226.0995 (observed). IR ($CHCl_3$): 1702, 1633 $cm^{-1}$.

*2.2.2. trans-N,N-Dimethyl-2-naphthylacrylamide (4)*

The ester **3** was hydrolyzed to the carboxylic acid. To 0.5 g of the acid, 30 ml of thionyl chloride was added and refluxed until the evolution of gas ceased (3 h). The excess thionyl chloride was evaporated under reduced pressure, and the residue, dissolved in 30 ml of anhydrous diethyl ether, was added to 0.43 g of dimethylammonium chloride. To this mixture, 3 ml of 3 M KOH was added dropwise at 0 °C and the resulting mixture was stirred overnight at room temperature. The organic layer was extracted with water, dried over $MgSO_4$ and the solvent was removed under vacuum. The residue was sublimated and recrystallized from hexane to afford **4** as a crystalline solid in 55% yield (m.p., 160–161 °C). $^1H$ NMR $\delta$: 7.94–7.50 (m, 7H), 7.70 (dd, $J=8.5$, 1.5 Hz, 1H), 7.02 (d, $J=15$ Hz, 1H), 3.23 (s, 3H), 3.10 (s, 3H). $^{13}C$ NMR (decoupled) $\delta$: 166.8, 142.5, 133.9, 133.4, 132.8, 129.3, 128.6, 128.5, 127.8, 126.9, 126.6, 123.7, 117.6, 37.5, 36.0. HRMS $m/z$: 225.1153 (calculated); 225.1151 (observed). IR ($CHCl_3$): 1649, 1605 $cm^{-1}$.

*2.2.3. trans-Ethyl-1-naphthylacrylate (5)*

Reaction of 1-naphthaldehyde (Aldrich) with (carboethoxymethyl)triphenylphosphonium bromide by the method described for the preparation of **3** provided **5** as a colorless oil in 65% yield (the methyl ester has been characterized previously [17]). $^1H$ NMR $\delta$: 8.54 (d, $J=15.9$ Hz, 1H), 8.21 (d, $J=8.3$ Hz, 1H), 7.90 (m, 2H), 7.76 (d, $J=7.2$ Hz, 1H), 7.54 (m, 3H), 6.54 (d, $J=15.7$ Hz, 1H), 4.33 (q, $J=7.1$ Hz, 2H), 1.39 (t, $J=7.1$ Hz, 3H). $^{13}C$ NMR (decoupled) $\delta$: 163.4, 141.6, 133.7, 131.8, 131.5, 130.6, 128.8, 126.9, 126.3, 125.6, 125.1, 123.5, 121.0, 60.7, 14.5. HRMS $m/z$: 226.0994 (calculated); 226.1007 (observed). IR ($CHCl_3$): 1706, 1637 $cm^{-1}$.

*2.2.4. Ethyl-3-(2-naphthyl)-3-diethylaminopropanoate (3a)*

Irradiation of **3** with diethylamine followed by chromatography afforded **3a** as a yellow oil in 42% yield. $^1H$ NMR $\delta$: 7.32–7.78 (m, 7H), 4.51 (t, $J=7.5$ Hz, 1H), 4.08 (q, $J=7.1$ Hz, 2H), 3.05 (dd, $J=15.1$, 7.5 Hz, 1H), 2.82 (dd, $J=14.8$, 8.0 Hz, 1H), 2.65 (m, 2H), 2.43 (m, 2H), 1.18 (t, $J=7.1$ Hz, 3H), 1.08 (t, $J=7.1$ Hz, 6H). $^{13}C$ NMR (decoupled) $\delta$: 172.7, 140.3, 133.6, 132.5, 128.2, 127.7, 127.6, 126.2, 126.0, 125.8, 125.4, 65.5, 60.2, 45.9, 40.6, 39.5, 14.2. HRMS $m/z$: 285.1729 (calculated); 285.1727 (observed) (major fragments (relative intensity): 240 (7), 154 (10), 58 (100)). IR ($CHCl_3$): 1722 $cm^{-1}$.

*2.2.5. Ethyl-3-(2-naphthyl)propanoate (3b)*

The above reaction also afforded **3b** as a yellow oil in 11% yield. $^1H$ NMR $\delta$: 7.84–7.27 (m, 7H), 4.13 (t, $J=7.1$ Hz, 2H), 3.13 (t, $J=7.7$ Hz, 2H), 2.72 (t, $J=7.7$ Hz, 2H), 1.24 (t, $J=7.1$ Hz, 3H). $^{13}C$ NMR (decoupled) $\delta$: 173.0, 138.1, 133.6, 132.2, 128.1, 127.7, 127.5, 127.1, 126.5, 126.1, 125.4, 60.5, 35.9, 31.2, 14.3. HRMS $m/z$: 228.1150 (calculated); 228.1149 (observed) (major fragments (relative intensity): 228 (9), 183 (19), 141 (71), 154 (100)). IR ($CHCl_3$): 1709 $cm^{-1}$.

*2.2.6. Ethyl-3-(2-naphthyl)-4-dimethylaminobutanoate (3d)*

Irradiation of **3** with trimethylamine followed by chromatography afforded **3d** as a yellow oil in 55% yield. $^1H$ NMR $\delta$: 7.81–7.35 (m, 7H), 4.01 (m, 2H), 3.51 (m, 1H), 2.91 (dd, $J=15.4$, 6.0 Hz, 1H), 2.62 (dd, $J=15.6$, 8.7 Hz, 1H), 2.54 (m, 1H), 2.26 (s, 6H), 1.11 (t, $J=7.1$ Hz, 3H). $^{13}C$ NMR (decoupled) $\delta$: 172.7, 140.3, 133.6, 132.5, 128.2, 127.7, 127.6, 126.2, 126.0, 125.8, 125.4, 65.5, 60.2, 45.9, 40.6, 39.5, 14.2. HRMS $m/z$: 285.1729 (calculated); 285.1727 (observed) (major fragments (relative intensity): 240 (7), 154 (10), 58 (100)). IR ($CHCl_3$): 1727 $cm^{-1}$.

*2.2.7. N,N-Dimethyl-3-(2-naphthyl)-3-diethylaminobutanamide (4a)*

Irradiation of **4** with diethylamine followed by chromatography afforded **4a** as a yellow oil in 29% yield. $^1H$ NMR $\delta$: 7.82–7.43 (m, 7H), 4.51 (m, 1H), 3.03 (m, 1H), 2.96 (m, 1H), 2.86 (s, 3H), 2.81 (s, 3H), 2.62 (m, 2H), 2.50 (m, 2H), 1.04 (t, $J=7.2$ Hz, 6H). $^{13}C$ NMR (decoupled) $\delta$: 171.4, 139.5, 133.2, 132.6, 128.0, 127.6, 127.5, 126.8, 126.6, 125.8, 125.5, 61.4, 43.4, 37.4, 36.4, 35.5, 12.7. HRMS $m/z$: 298.2045 (calculated); 298.2048 (observed) (major fragments (relative intensity): 269 (70), 212 (84), 72 (100)). IR ($CHCl_3$): 1714 $cm^{-1}$.

*2.2.8. N,N-Dimethyl-3-(2-naphthyl)propanamide (4b)*

The above reaction also afforded **4b** as a yellow oil in 11% yield. $^1H$ NMR $\delta$: 7.82–7.36 (m, 7H), 3.14 (t, $J=8.0$ Hz, 2H), 2.97 (s, 3H), 2.95 (s, 3H), 2.71 (t, $J=7.8$ Hz, 2H). HRMS $m/z$: 227.1310 (calculated); 227.1312 (observed) (major fragments (relative intensity): 227 (100), 154 (95), 141 (67)). IR ($CHCl_3$): 1706 $cm^{-1}$.

*2.2.9. N,N-Dimethyl-3-(2-naphthyl)-4-dimethylaminopropanamide (4d)*

Irradiation of **4** with trimethylamine followed by chromatography afforded **4d** as a yellow oil in 32% yield. $^1H$ NMR $\delta$: 7.81–7.43 (m, 7H), 3.66 (m, 1H), 2.87 (s, 3H), 2.84 (s, 3H), 2.66 (m, 4H), 2.27 (s, 6H). $^{13}C$ NMR (decoupled) $\delta$: 171.8, 141.2, 133.6, 132.5, 128.1, 127.7, 127.6, 126.2, 126.1, 125.9, 125.4, 65.1, 45.9, 40.3, 37.9, 37.3, 35.5. HRMS $m/z$: 284.1889 (calculated); 284.1899 (observed) (major fragments (relative intensity): 154 (9), 72 (11), 58 (100)). IR ($CHCl_3$): 1713 $cm^{-1}$.

*2.2.10. Ethyl-3-(1-naphthyl)-3-diethylaminopropanoate (5a)*

Irradiation of **5** with diethylamine followed by chromatography afforded **5a** as a yellow oil in 40% yield. $^1H$ NMR $\delta$: 8.50 (d, $J=8.2$ Hz, 1H), 7.84 (d, $J=7.7$ Hz, 1H), 7.75 (d,

$J$ = 8.0 Hz, 1H), 7.52–7.39 (m, 4H), 5.08 (m, 1H), 3.95 (q, $J$ = 7.1 Hz, 2H), 3.05 (dd, $J$ = 14.5, 6.0 Hz, 1H), 2.88 (dd, $J$ = 14.8, 8.7 Hz, 1H), 2.61 (m, 4H), 1.01 (m, 9H). $^{13}$C NMR (decoupled) $\delta$: 172.4, 137.3, 134.0, 132.4, 128.6, 127.9, 125.6, 125.4, 125.1, 124.9, 124.6, 60.3, 58.2, 43.5, 36.5, 14.0, 13.0. HRMS $m/z$: 299.1885 (calculated); 299.1884 (observed) (major fragments (relative intensity): 212 (100), 185 (14), 153 (21)). IR ($CHCl_3$): 1726 cm$^{-1}$.

*2.2.11. Ethyl-3-(1-naphthyl)propanoate (5b)*

Also obtained in the above reaction was **5b** as a yellow oil in 15% yield. $^1$H NMR $\delta$: 8.05 (d, $J$ = 8.0 Hz, 1H), 7.87 (d, $J$ = 8.0 Hz, 1H), 7.74 (d, $J$ = 7.7 Hz, 1H), 7.56–7.35 (m, 4H), 4.16 (q, $J$ = 7.1 Hz, 2H), 3.43 (t, $J$ = 8.0 Hz, 2H), 2.76 (t, $J$ = 8.0 Hz, 2H), 1.26 (t, $J$ = 7.1 Hz, 3H). $^{13}$C NMR (decoupled) $\delta$: 173.1, 136.6, 133.9, 131.6, 128.9, 127.1, 126.1, 126.0, 125.6, 123.5, 60.6, 35.4, 28.2, 14.3. HRMS $m/z$: 285.1150 (calculated); 285.1141 (observed) (major fragments (relative intensity): 228 (83), 154 (93), 141 (100)). IR ($CHCl_3$): 1720 cm$^{-1}$.

*2.2.12. Ethyl-3-(1-naphthyl)-4-dimethylaminobutanoate (5d)*

Irradiation of **5** with trimethylamine followed by chromatography afforded **5d** as a yellow oil in 52% yield. $^1$H NMR $\delta$: 8.22 (d, $J$ = 8.2 Hz, 1H), 7.85 (d, $J$ = 8.0 Hz, 1H), 7.73 (d, $J$ = 8.0 Hz, 1H), 7.58–7.35 (m, 4H), 4.28 (m, 1H), 4.00 (m, 2H), 2.97 (dd, $J$ = 15.5, 7.0 Hz, 1H), 2.74 (dd, $J$ = 15.5, 7.4 Hz, 1H), 2.56 (m, 2H), 2.29 (s, 6H), 1.09 (t, $J$ = 7.1 Hz, 3H). $^{13}$C NMR (decoupled) $\delta$: 172.8, 138.9, 134.0, 131.7, 129.0, 127.2, 126.1, 125.5, 123.3, 123.0, 65.5, 60.2, 59.1, 45.9, 39.6, 14.1. HRMS $m/z$: 285.1729 (calculated); 285.1735 (observed) (major fragments (relative intensity): 153 (13), 98 (22), 58 (100)). IR ($CHCl_3$): 1726 cm$^{-1}$.

## 3. Results and discussion

### 3.1. Ground state conformation

The ground state conformation of **2** has been investigated by both experimental and computational methods. The solution phase conformations of **2** have been the subject of several NMR investigations which have yielded conflicting results concerning the lowest energy conformation [18]. We have investigated the ground state conformations of **2** by NOE difference experiments in $CDCl_3$ solution (Fig. 1). The larger NOEs for $H_1 - H_\alpha$ vs. $H_1 - H_\beta$ and for $H_3 - H_\beta$ vs. $H_3 - H_\alpha$ indicate that a-**2** is the lowest energy conformation in solution. Gustav and Schreiber [7] proposed, on the basis of PPP-CI calculations, that both the ground and excited states of s-**2** and a-**2** are planar and that their spectroscopic properties should be very similar. Pfanstiel and Pratt [8] found the ground state of a-**2** to lie 239 cm$^{-1}$ below s-**2** on the basis of Hartree–Fock calculations (Gaussian 90, 6-31G* basis set). Their minimized geometry for a-**2** was planar, whereas the calculated geometry of s-**2** was non-planar, with a naphthyl–vinyl dihedral angle of 30°. Their spectroscopic results indicated that both conformers were planar in the $S_0$ and $S_1$ states. The lower ground state energy of a-**2** relative to s-**2** is consistent with the stronger origin band for a-**2**.

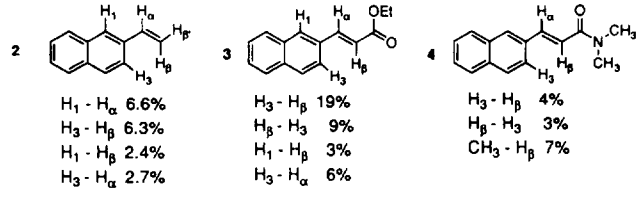


Fig. 1. NOE data for 2-vinylnaphthalene **2**, ester **3** and amide **4**.

The naphthylacrylic acid derivatives **3–5** can exist as mixtures of up to four conformers due to rotation about both the naphthyl–vinyl and enone single bonds. Enone conformations can be assigned on the basis of the relative intensities of IR $\nu_{C=C}$ vs. $\nu_{C=O}$ bands, as described by Kronenberg and Havinga [19]. We have previously used this method to assign an s-*trans*-enone conformation to cinnamate esters and an s-*trans*-enone conformation to cinnanamides [20]. IR data (see Section 2) for **3–5** support analogous assignments of s-*trans*-enone conformations to esters **3** and **5** and an s-*cis*-enone conformation to amide **4**. NOE difference experiments (Fig. 1) provide additional information about the ground state conformations of **3** and **4**. The results for **3** are similar to those for **2**. The more limited data for **4** display only those NOEs expected for the s-*trans*-naphthyl-vinyl conformer and confirm the s-*cis*-enone assignment based on IR spectroscopy. In analogy with other 1-vinylnaphthalenes [1], **5** is assumed to exist as the s-*trans*-naphthyl-vinyl conformer.

The conformational energies of the four possible conformers of **3–5** were also investigated by molecular modeling using a modified MM2 force field as supplied in the CHEM 3D PLUS software package [15]. The calculated energies of the s-*trans*-enone conformers of **3** and **5** are approximately 2 kcal mol$^{-1}$ below the s-*cis*-enone conformers and the s-*cis*-enone conformer of **4** is approximately 3 kcal mol$^{-1}$ below the s-*trans*-enone conformer. The minimized geometries of a-**3** and a-**4** are planar, whereas the minimized geometries of s-**3** and s-**4** have naphthyl–vinyl dihedral angles of approximately 30°, similar to that reported for s-**2** [8]. The calculated difference in energy between a-**3** and s-**3** ($\Delta G$ = 0.02 kcal mol$^{-1}$) is smaller than that between a-**4** and s-**4** ($\Delta G$ = 0.1 kcal mol$^{-1}$). Saltiel et al. [2] have determined the ratio of the ground state conformers for **1** (s-**1**/a-**1** = 0.45) based on the resolved absorption spectra of the two isomers. Resolved spectra are not available for the conformers of **2–4** (see below). Rough estimates of the conformer ratios obtained from the NOE data in Fig. 1 are s-**2**/a-**2** and s-**3**/a-**3** ~ 0.33 and s-**4**/a-**4** < 0.1. The smaller value for **4** relative to **3** is consistent with the results of MM2 modeling, and may reflect the combined effects of non-bonded repulsion between the β-vinyl hydrogen and aromatic $H_1$ and the methyl group anti to the carbonyl nitrogen (Fig. 1).

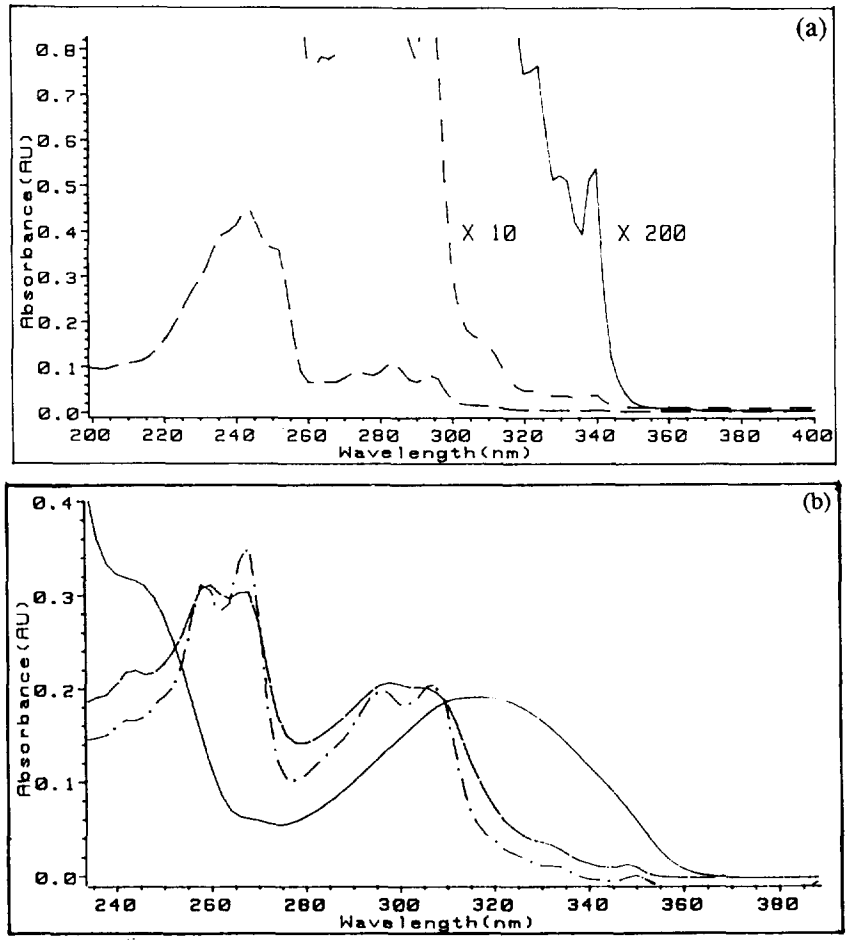


Fig. 2. UV spectra of $1.2\times10^{-5}$ M 2-vinylnaphthalene **2** (a) and $1.2\times10^{-5}$ M **3** (– · –), $3.2\times10^{-5}$ M **4** (– – –) and $1.7\times10^{-5}$ M **5** (———) (b) in hexane solution.

### 3.2. *Absorption spectra*

The electronic absorption spectra of **2–5** in hexane solution are shown in Fig. 2(a) and (b). The spectrum of **2** displays bands of low, medium and high intensity, all of which have vibrational structure. The spectra of **3** and **4** are similar to that of **2**, with maxima shifted to longer wavelength in the order **3** > **4** > **2**. The same order is observed for the molar absorbance of the long-wavelength absorption band. The spectrum of **5** is markedly different from those of **2–4**, displaying a single broad long-wavelength absorption band. Spectra recorded in diethyl ether or acetonitrile solution display neither solvent-induced shifts nor significant broadening. The absorption data for **2–5** in hexane and acetonitrile solution are summarized in Table 1.

The electronic structure and spectra of **2–5** have been investigated by semiempirical INDO/S-SCF-CI (ZINDO) calculations using the algorithm developed by Zerner and coworkers [13]. The molecular structures were obtained from MM2 calculations [15]. The nodal patterns of the frontier orbitals ($\pi$ and $\pi^*$) of a-**2** and s-**2** are similar to those for a-**2** derived from 6-31G* calculations [8]. The nodal patterns for the four or five highest energy occupied (HOMO) and two lowest energy unoccupied (LUMO) orbitals of a-**3** and a-**4** are shown in Fig. 3. Similar nodal patterns and orbital energies were calculated for s-**3** and s-**4** respectively. As noted by Pfanstiel and Pratt [8] in the case of **2**, the nodal patterns of **3** and **4** are different from those for ordinary substituted naphthalenes due to extensive delocalization into the vinyl group. The nodal patterns of the $\pi$ orbitals of **3** and **4** are similar to those of **2**; however, the $\pi^*$ orbitals of **3** and **4** display more conjugation, involving the carbonyl orbitals. The $\pi$ orbitals of **5** more closely resemble those of naphthalene. The oxygen n orbitals of **3–5** lie below the highest occupied $\pi$ orbitals, as does the amide $\pi$ orbital of **4**.

Table 1
UV absorption data for naphthalene derivatives

| Naphthalene | Solvent | $\lambda_1$ ($\varepsilon$) | $\lambda_2$ ($\varepsilon$) | $\lambda_2$ ($\varepsilon$) |
|---|---|---|---|---|
| 2 | Hexane | 340 (186) | 284 (8920) | 244 (37000) |
| 3 | Hexane | 350 (1700) | 308 (16000) | 268 (26800) |
| 3 | Acetonitrile | 350 (1400) | 308 (18000) | 268 (27500) |
| 4 | Hexane | 348 (428) | 298 (6020) | 260 (9360) |
| 4 | Acetonitrile | 348 (579) | 298 (6880) | 260 (10000) |
| 5 | Hexane | 316 (10400) | 246 (16990) | |
| 5 | Acetonitrile | 316 (8740) | 246 (15600) | |

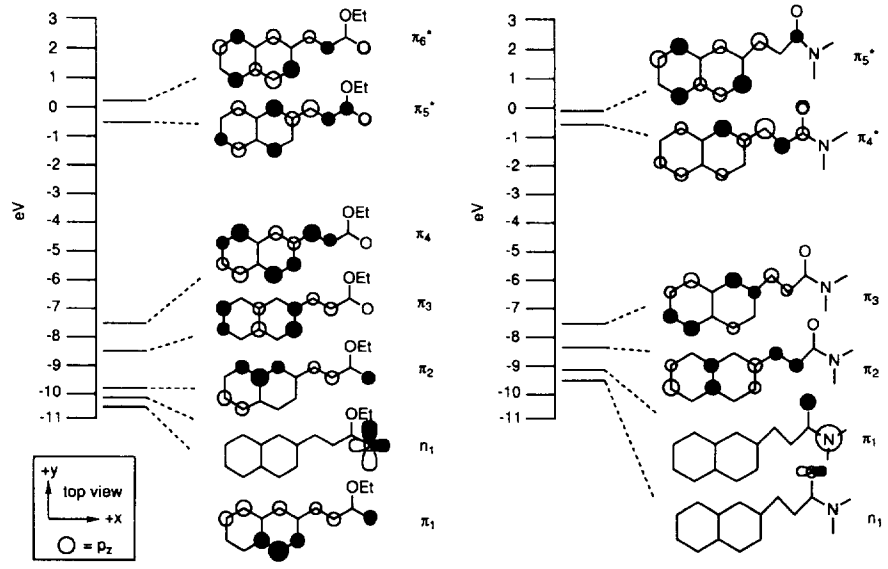


Fig. 3. ZINDO calculated frontier molecular orbitals for a-**3** and a-**4**.

The calculated absorption maxima, oscillator strengths and character of selected excited singlet states of **2**–**5** are summarized in Table 2. Both a-**2** and s-**2** exhibit three well-separated $\pi,\pi^*$ transitions of low, medium and high oscillator strength, in good agreement with the observed spectrum (Fig. 2(a)). All three of these transitions involve orbitals with extended conjugation, and thus it is not surprising that they lie at lower energy than the three lowest energy transitions of naphthalene. The first and third $\pi,\pi^*$ transitions result from configuration interaction of the HOMO → SLUMO and SHOMO → LUMO transitions. This situation is analogous to the four-level model developed by Platt [21] for naphthalene and other aromatic hydrocarbons. The different oscillator strengths for $S_1$ and $S_3$ result from the stealing of intensity by the higher energy transition. Intermediate in energy is a $\pi,\pi^*$ transition of largely HOMO → LUMO character with an intermediate oscillator strength. Contrary to the assumption of Pfanstiel and Pratt [8], $S_1$ does not arise from a HOMO → LUMO transition.

The calculated energies for the lowest energy $\pi,\pi^*$ transitions of a-**2** and s-**2** are essentially identical, in agreement with the observation of two electronic origins in the fluores-

Table 2
Calculated absorption maxima ($\lambda_{max}$), oscillator strengths ($f$) and character of the excited singlet states ($S_n$) of naphthalene derivatives

| Naphthalene | State | $\lambda_{max}$ (nm) | $f$ | Character, CI |
|---|---|---|---|---|
| s-**2** | $S_1$ | 325.4 | 0.0024 | $\pi,\pi^*$: 41% SHOMO → LUMO, 49% HOMO → SLUMO |
| | $S_2$ | 289.4 | 0.239 | $\pi,\pi^*$: 91% HOMO → LUMO |
| | $S_3$ | 247.4 | 1.58 | $\pi,\pi^*$: 47% SHOMO → LUMO, 41% HOMO → SLUMO |
| a-**2** | $S_1$ | 325.8 | 0.0022 | $\pi,\pi^*$: 41% SHOMO → LUMO, 49% HOMO → SLUMO |
| | $S_2$ | 289.3 | 0.237 | $\pi,\pi^*$: 91% HOMO → LUMO |
| | $S_3$ | 247.4 | 1.57 | $\pi,\pi^*$: 47% SHOMO → LUMO, 41% HOMO → SLUMO |
| s-**3** | $S_1$ | 345 | 0.001 | $n,\pi^*$: 42% n → LUMO |
| | $S_2$ | 334 | 0.047 | $\pi,\pi^*$: 20% SHOMO → LUMO, 20% HOMO → SLUMO |
| | $S_3$ | 306 | 0.243 | $\pi,\pi^*$: 67% HOMO → LUMO |
| | $S_4$ | 267 | 1.19 | $\pi,\pi^*$: 28% SHOMO → LUMO, 57% HOMO → SLUMO |
| a-**3** | $S_1$ | 345 | 0.001 | $n,\pi^*$: 41% n → LUMO |
| | $S_2$ | 333 | 0.046 | $\pi,\pi^*$: 23% SHOMO → LUMO, 20% HOMO → SLUMO |
| | $S_3$ | 299 | 0.423 | $\pi,\pi^*$: 67% HOMO → LUMO |
| | $S_4$ | 267 | 1.27 | $\pi,\pi^*$: 35% SHOMO → LUMO, 53% HOMO → SLUMO |
| s-**4** | $S_1$ | 365 | 0.001 | $n,\pi^*$: 47% n → LUMO |
| | $S_2$ | 336 | 0.110 | $\pi,\pi^*$: 30% SHOMO → LUMO, 30% HOMO → LUMO |
| | $S_3$ | 316 | 0.446 | $\pi,\pi^*$: 62% HOMO → LUMO |
| | $S_4$ | 275 | 1.10 | $\pi,\pi^*$: 32% SHOMO → LUMO, 54% HOMO → SLUMO |
| a-**4** | $S_1$ | 385 | 0.001 | $n,\pi^*$: 48% n → LUMO |
| | $S_2$ | 331 | 0.075 | $\pi,\pi^*$: 22% SHOMO → LUMO, 25% HOMO → SLUMO |
| | $S_3$ | 300 | 0.473 | $\pi,\pi^*$: 67% HOMO → LUMO |
| | $S_4$ | 270 | 1.27 | $\pi,\pi^*$: 37% SHOMO → LUMO, 50% HOMO → SLUMO |
| **5** | $S_1$ | 348 | 0.001 | $n,\pi^*$: 36% n → LUMO, 34% n → SLUMO |
| | $S_2$ | 338 | 0.545 | $\pi,\pi^*$: 74% HOMO → LUMO |

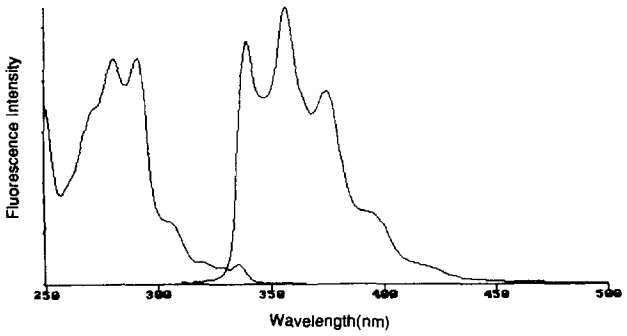


Fig. 4. Fluorescence emission and excitation spectra of 2-vinylnaphthalene **2** in hexane solution.

cence excitation spectrum of **2** in a supersonic jet which are separated by only 16 $cm^{-1}$ [8]. The observed ratio of the band intensities [8] is also comparable with the isomer ratio estimated from NOE data (Fig. 1). The description of the two lowest singlet states of a-**2**, provided by ZINDO calculations, is similar to that reported by Bartocci et al. [3] for CNDO/S calculations for a-**1**. Whereas the lowest singlet states of a-**2** and s-**2** are predicted to have similar energies, oscillator strengths and configuration interaction (Table 2), CNDO/S calculations indicate that this is not the case for s-**1** and a-**1** [3]. These calculations have been used to rationalize the different electronic spectra observed for s-**1** and a-**1** [1,2].

The calculated spectra of **3** and **4** display three $\pi,\pi^*$ transitions similar to those of **2**, but with more extensive configuration interaction (Table 2). As in the case of **2**, there are only minor differences in the calculated spectra of a-**3** and s-**3**; however, the differences are more significant for a-**4** and s-**4**. The calculated spectrum of **5** differs significantly from those of the other naphthalene derivatives. Its lowest energy $\pi,\pi^*$ transition is largely HOMO → LUMO in character and of moderately large oscillator strength. Similar results have been reported for *trans*-1-(1-naphthyl)-2-phenylethene [3]. In addition to the three $\pi,\pi^*$ transitions described above, ZINDO calculations for **3**–**5** indicate the presence of $n,\pi^*$ transitions of very low oscillator strength at energies slightly below the lowest $\pi,\pi^*$ transitions. The $n,\pi^*$ states have extensive configuration interaction involving all of the low-energy $\pi^*$ orbitals. ZINDO does not provide reliable energies in such cases and thus the $n,\pi^*$ states may actually lie above the lowest $\pi,\pi^*$ states [14].

### 3.3. Fluorescence

The fluorescence emission and excitation spectra of **2** in hexane solution are shown in Fig. 4. The lowest energy emission maximum lies near the gas phase origins for a-**2** (334.9 nm) and s-**2** (334.7 nm). The appearance of the emission spectrum is independent of the solvent polarity. Structured fluorescence emission and excitation spectra similar to those of **2** are observed for **3** and **4** in hexane solution. The small Stokes shifts for **2**–**4** are consistent with a planar geometry for both $S_0$ and $S_1$. The fluorescence emission spectrum of **5** is weakly structured in hexane solution. The emission spectra of **2**, **3** and **5** display little or no dependence on the excitation wavelength. The emission spectrum of **4** is excitation wavelength dependent. The emission maxima for **2** in hexane solution and for **3**–**5** in hexane, diethyl ether and acetonitrile solution are reported in Table 3. The emission spectra of **3**–**5** broaden and shift to the red in more polar solvents, indicative of an increase in polarity for $S_1$ vs. $S_0$. Similar solvent

Table 3
Fluorescence and photoisomerization data[a]

| Naphthalene | Solvent | $\lambda_{max}$ (nm)[b] | $\Phi_f^c$ | $\tau_1$ (ns) (A)[d] | $\tau_2$ (ns) (A)[e] | $\Phi_t^f$ |
|---|---|---|---|---|---|---|
| **2** | Hexane | 340, 357 | 0.32 | 105 (0.92) | 37.3 (0.08) | |
| **3** | Hexane | 354, 373 | 0.69 | 22.9 (0.87) | 9.0 (0.13) | 0.16 |
| **3** | Cyclohexane[g] | | 0.61 | | | 0.22 |
| **3** | Ether | 356, 374 | 0.58 | 16.7 (0.84) | 5.0 (0.16) | |
| **3** | Acetonitrile | 388 | 0.41 | 8.4 (0.77) | 2.0 (0.23) | 0.30 |
| **3** | Methanol[g] | | 0.39 | | | 0.37 |
| **4** | Hexane | 352, 371 | 0.01 | 0.10 (0.97) | 14.5 (0.03) | 0.05 |
| **4** | Ether | 356, 372 | 0.01 | 0.22 (0.98) | 13.0 (0.02) | 0.17 |
| **4** | Acetonitrile | 377 | 0.01 | 0.18 (0.99) | 7.6 (0.01) | 0.32 |
| **5** | Hexane | 374 | 0.03 | 0.8 (1.00) | | 0.14 |
| **5** | Cyclohexane[g] | | 0.05 | | | 0.19 |
| **5** | Ether | 382 | 0.03 | 0.8 (1.00) | | |
| **5** | Acetonitrile | 402 | 0.03 | 0.8 (1.00) | | 0.23 |
| **5** | Methanol[g] | | 0.05 | | | 0.22 |

[a]Data for nitrogen- or argon-purged solutions.
[b]Wavelengths of two highest energy maxima reported when observed.
[c]Fluorescence quantum yield relative to pyrene [10].
[d]Fluorescence decay times (and pre-exponentials) assigned to the major (anti) conformer.
[e]Fluorescence decay times (and pre-exponentials) assigned to the minor (syn) conformer.
[f]Quantum yield for the formation of the cis isomer determined by GC analysis at low conversions.
[g]Data from Ref. [9].

shifts have been reported by Costa et al. [22] for benzyl-2-naphthoate and benzyl-1-naphthoate. Inspection of the frontier orbitals in Fig. 3 indicates that the lowest singlets of **3–5** have partial charge transfer (vinylnaphthalene → acrylate) character which may account for the observed solvent dependence.

The fluorescence decay times ($\tau$) and pre-exponentials ($A$) for **2–5** in hexane, ether and acetonitrile are also reported in Table 3. Decay profiles were obtained using a single-photon counting apparatus with a time resolution of approximately 0.2 ns, and the decays were deconvoluted using a single- or multi-exponential least-squares analysis, as described by James et al. [11]. Data for **4** were obtained using an apparatus with a time resolution of approximately 50 ps. Samples were excited at 303 nm and fluorescence decay was monitored near the emission maximum (Table 2). Satisfactory fits to a single exponential were obtained for **5** and to a double exponential for **2–4**. The goodness of fit was judged by the randomness of the residuals, autocorrelation function and reduced $\chi^2$ values (less than 1.2). The decay times for **3** and **4** are independent of the excitation or emission wavelength. The pre-exponentials for **3** display only slight excitation wavelength dependence, whereas those for **4** are more strongly dependent on the excitation wavelength. On cooling methylcyclohexane solutions of **3** or **4** from room temperature (298 K) to 150 K, modest red shifts (approximately 1–2 nm) and slight broadening of the emission spectra are observed. The lifetimes and pre-exponentials vary only slightly with decreasing temperature.

By analogy with the photophysical behavior of **1** and other 2-arylvinylnaphthalenes [1], the dual emission observed for **2–4** is attributed to emission from the syn and anti conformers. Single-exponential decay is observed for **5** and other 1-vinylnaphthalenes, which exist as a single conformer [1]. The shorter lifetimes and lower fluorescence quantum yields for 1- vs. 2-vinylnaphthalenes are due to the different character of their fluorescent singlet states [23]. The longer lived fluorescence components account for approximately 75% of the total fluorescence of **1**, 90% of the fluorescence of **2** and 80% of the fluorescence of **3** in hexane solution. The assignment of this component to the anti conformers of **2** and **3** is consistent with previous assignments for **1** [2] and the results of NOE studies (Fig. 1). The absence of significant excitation wavelength-dependent fluorescence from **2** and **3** may reflect the domination of the emission by a single conformer as well as the overlapping of the spectra for the two conformers.

Also reported in Table 3 are the quantum yields of fluorescence $\Phi_f$ of **2–5** in several solvents, together with the values for **3** and **5** previously reported by Tanaka et al. [9]. The values of $\Phi_f$ for **4** and **5** are significantly smaller than those for **2** and **3**. The low value of $\Phi_f$ for **4** discouraged efforts to resolve the fluorescence spectra of the syn and anti conformers. Approximate fluorescence quantum yields for the two conformers of **3** can be calculated from the ground state populations (estimated from NOE data), contributions to the total fluorescence and the total fluorescence quantum yield (Table 3). The resulting values are $\Phi_f \sim 0.4$ for s-**3** and $\Phi_f \sim 0.9$ for a-**3**. These values and the fluorescence lifetimes (Table 3) can be used to calculate approximate fluorescence rate constants ($k_f = \Phi_f \tau^{-1}$). The calculated values of $k_f \sim 3 \times 10^7\ s^{-1}$ for s-**3** and $4 \times 10^7\ s^{-1}$ for a-**3** are essentially the same, in accord with the similar character of the lowest singlet states of s-**3** and a-**3** (Table 2).

The absorption and fluorescence spectra of **4** in hexane solution resemble those of **2** and **3**. However, the fluorescence quantum yield of **4** is much smaller than those of **2** or **3**. Furthermore, one of the fluorescence decay times of **4** is much shorter than either of the decay times of **2** or **3** (Table 3). These observations can be rationalized by the assignment of the very short-lived fluorescence to the major conformer a-**4** and the long-lived fluorescence to the minor conformer s-**4**. Assuming a value of $k_f$ for s-**4** similar to that for s-**3**, the fluorescence quantum yield for s-**4** should be $\Phi_f = k_f \tau^{-1} = 0.44$. Since the observed total fluorescence quantum yield for **4** is only approximately 0.01, the ground state population of s-**4** can be no more than 2%, in accord with the upper limit of 10% estimated from the NOE data (Fig. 1).

This analysis leaves unanswered the question of why the lifetime of a-**4** is anomalously short. A plausible explanation may be provided by the existence of a singlet n,π* state at lower energy than the π,π* state, as suggested by the ZINDO calculations (Table 2). A similar explanation has been used to account for the very short fluorescence decay times of methyl cinnamate and α-pyridylpyrrolinones [24] and the absence of fluorescence from 3-(2-pyridyl)propenamides [25]. Rapid internal conversion from the initially populated fluorescent π,π* state to a lower energy non-fluorescent n,π* state may account for the short lifetime and the low fluorescence quantum yield of a-**4** (Table 3). Both the appearance of the fluorescence spectrum and the value of $k_f \sim 5 \times 10^7\ s^{-1}$ estimated for a-**4** are indicative of emission from a π,π* state rather than an n,π* state. As noted above, ZINDO calculations do not provide accurate energies for states with extensive configuration interaction, such as the n,π* states of **3–5**. The calculated separation of π,π* and n,π* states is larger for a-**4** than for s-**4** or the two conformers of **3**. Thus it is possible that the n,π* state lies below the fluorescent π,π* state only in the case of a-**4**. Mixing of the singlet π,π* and n,π* states may also account for the shorter singlet lifetimes of **3** and **4** vs. **2**.

### 3.4. Photoisomerization

The photoisomerization of **3** and **5** has previously been investigated by Tanaka et al. [9]. They observed that the quantum yields of trans → cis photoisomerization ($\Phi_i$) increase with increasing solvent polarity. Our values of $\Phi_i$ for **3–5** in hexane and acetonitrile solution are reported in Table 3, together with the values of Tanaka et al. for **3** and **5** in cyclohexane and methanol solution. A triplet mechanism for photoisomerization was proposed by Tanaka et al. [9] on

Table 4
Quenching of the long-lived and short-lived fluorescence of ethyl-2-naphthylacrylate (3) by triethylamine and diethylamine

| Amine | Solvent | Component | $K_{SV}$ ($M^{-1}$)[a] | $10^{-9}k_q$ ($M^{-1}$ $s^{-1}$)[b] |
|---|---|---|---|---|
| $Et_3N$ | Hexane | Long | 415 | 18 |
| | | Short | 276 | 31 |
| | Ether | Long | 235 | 14 |
| | | Short | 183 | 36 |
| | Acetonitrile | Long | 123 | 15 |
| | | Short | 48 | 24 |
| $Et_2NH$ | Hexane | Long | 272 | 12 |
| | | Short | 260 | 29 |
| | Ether | Long | 156 | 9 |
| | | Short | 93 | 19 |
| | Acetonitrile | Long | 88 | 19 |
| | | Short | 30 | 15 |

[a]Slope of linear Stern–Volmer plot for reduction of the singlet lifetime of **2** by added amine at room temperature in nitrogen-purged solutions.
[b]Calculated from $K_{SV}$ and the lifetime data in Table 3.

the basis of enhanced isomerization in the presence of oxygen or propyl bromide and triplet sensitization using Michler's ketone. The observation of temperature-independent fluorescence lifetimes for s-**3** and a-**3** provides evidence against a singlet mechanism [26]. A triplet mechanism is also consistent with the solvent dependence of $\Phi_i$ and the singlet lifetimes of **3** (Table 3). An increase in the rate constant for intersystem crossing in polar solvents may account for both the decrease in $\tau$ and the increase in $\Phi_i$.

The mechanism of photoisomerization of **1** has been the subject of some controversy [1,2]. Saltiel et al. [2] concluded that it occurs predominantly via a singlet state mechanism. A modest increase in either the barrier for singlet state isomerization or the rate constant for intersystem crossing may account for the observation of similar fluorescence decay times but different isomerization mechanisms for **1** and **3**.

Assuming that the quantum yield for triplet state isomerization is approximately 0.5, the quantum yield for intersystem crossing should be approximately double the measured value of $\Phi_i$. In the case of **3**, the sum of $\Phi_f + 2\Phi_i \sim 1.0$ (Table 3), thus accounting for all of the excited singlets. Much smaller values for this sum are observed for **4** and **5**. The very low value for **4** in hexane solution indicates that the short singlet lifetime of the predominant conformer, a-**4**, probably results from rapid internal conversion rather than singlet state isomerization or intersystem crossing. The syn and anti conformers of **3** and **4** have different lifetimes, and thus may be expected to have different photoisomerization quantum yields, as is the case for the syn and anti conformers of 2-(2-(2-pyridyl)ethenyl)indole [4]. Unfortunately, the similar absorption spectra of the syn and anti conformers preclude direct measurement of their independent $\Phi_i$ values.

### 3.5. Singlet quenching by amines

The fluorescence of **1** and other arylethenes and 1,2-diarylethenes is quenched by added amines [27–29]. Fluorescence quenching is proposed to occur via an electron transfer mechanism and, in some cases, is accompanied by the appearance of exciplex fluorescence. Saltiel et al. [5] have recently succeeded in resolving the formation and decay of the exciplexes of s-**1** and a-**1** with $Bu_3N$. The fluorescence of **3–5** is quenched by added $Et_2NH$ or $Et_3N$; however, no exciplex emission is observed. Stern–Volmer quenching constants $K_{SV}$, obtained from the slopes of linear plots of $\tau^0/\tau$ vs. [amine], for the quenching of the long-lived and short-lived components of **3** in hexane, ether and acetonitrile solution are reported in Table 4. Values of $k_q$ calculated from $K_{SV}$ and the measured value of $\tau^0$ are near the rate of diffusion in these non-viscous solvents ($k_{diff} \sim 3 \times 10^{10}$ $M^{-1}$ $s^{-1}$). Free energies for electron transfer quenching can be calculated from the singlet energies and reduction potentials of **3–5** ( −1.43, −1.59 and −1.41 V respectively) and the amine oxidation potentials using Weller's equation

$$\Delta G_{et} = E_D^{ox} - E_A^{red} - E_S + C$$

where $C$ is an empirical solvent constant ( −0.54 eV in hexane and −0.06 eV in acetonitrile [30]). The resulting values of $\Delta G_{et}$ are exergonic even in non-polar solvents.

For most combinations of solvent and amine, the value of $k_q$ is larger for the quenching of s-**3** vs. a-**3** (Table 4). Saltiel et al. [5] have also observed different values of $k_q$ for quenching of s-**1** vs. a-**1** by $Bu_3N$. Stern–Volmer plots for the quenching of the fluorescence intensity of **3** and **5** by added $Et_3N$ are linear for up to 90% quenching. In contrast, downward curvature is observed for the quenching of **4** by $Et_3N$ in hexane solution. The large difference in the singlet lifetimes for s-**4** and a-**4**, and their similar contributions to the total fluorescence, may account for the observation of curved Stern–Volmer plots.

Quenching of arylethenes and 1,2-diarylethenes by amine can result in 1,2-addition of the amine to the arylethene [28,29]. Preparative irradiation of **3** with $Et_2NH$ leads to the formation of adduct **3a** and the reduction product **3b**. Both products are presumed to be formed via electron transfer, followed by N–H proton transfer, to yield a radical pair which

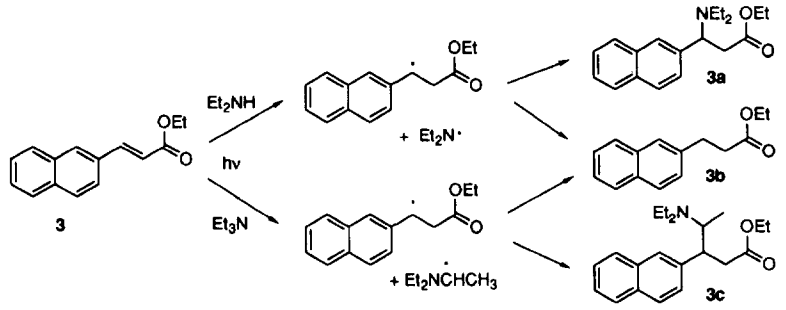


Scheme 1.

Table 5
Quantum yields for amine adduct and reduction product formation[a]

| Naphthalene | Solvent | $\Phi_{add}(Et_2NH)$ | $\Phi_{rdn}(Et_2NH)$ | $\Phi_{add}(Et_3N)$ |
|---|---|---|---|---|
| 3 | Hexane | 0.37 | 0.11 | 0.69 |
| 3 | Acetonitrile | 0.08 | 0.04 | 0.15 |
| 4 | Benzene | 0.13 | 0.08 | 0.17 |
| 4 | Acetonitrile | 0.05 | 0.06 | 0.07 |
| 5 | Hexane | 0.11 | 0.04 | 0.02 |
| 5 | Acetonitrile | 0.008 | 0.002 | 0.003 |

[a]Quantum yields determined at low conversion of naphthalene derivative in nitrogen-purged solutions containing sufficient amine for more than 90% quenching of naphthalene fluorescence.

can combine to yield **3a** and disproportionate to yield **3b** (Scheme 1). Irradiation of **3** with $Et_3N$ also yields both adduct **3c** (mixture of diastereomers) and **3b**. Takamuku et al. [31] previously observed the formation of **3b** and **3c** on irradiation of the photodimer of **3** with $Et_3N$. The reaction of **2** with $Et_3N$ to yield an adduct analogous to **3c** has been observed by Shirota [32]. The mechanism of $Et_3N$ addition requires α-C–H rather than N–H transfer, but is otherwise analogous to that for $Et_2NH$. The mixture of diastereomeric adducts formed with $Et_3N$ could not be separated. However, the single adduct **3d** formed in the reaction of **3** with $Me_3N$ was isolated and characterized. Adducts analogous to **3a** and **3d** were also formed on irradiation of **4** and **5** with $Et_2NH$ and $Me_3N$ respectively. Addition of both $Et_2NH$ and $Me_3N$ is highly regioselective, yielding only adducts in which H adds selectively to the ethene carbon adjacent to the carbonyl group. Adducts were characterized by $^1H$ and $^{13}C$ NMR and HRMS (see Section 2).

Quantum yields of adduct formation ($\Phi_{add}$) of **3–5** with $Et_2NH$ and $Et_3N$ were determined by GC analysis at low conversions (less than 10%) of the starting materials **3–5**. Values of $\Phi_{add}$ increase with increasing amine concentration, in accord with the usual singlet state mechanism for amine addition to arylethenes [28]. Values of $\Phi_{add}$ obtained in hexane and acetonitrile solution using amine concentrations sufficient to quench more than 90% of singlet **5** and the shorter lived conformers of **3** and **4** are summarized in Table 5. Values of $\Phi_{add}$ are smaller for **5** relative to **3** and **4**, possibly reflecting differences in the configuration of the reactive $\pi,\pi^*$ states (Table 2). Increasing solvent polarity results in a decrease in $\Phi_{add}$. This change may reflect a solvent-induced decrease in the exciplex lifetime, resulting from increased rate constants for intersystem crossing, non-radiative decay or solvation, to yield non-reactive solvent-separated radical ions. It is also possible that the exciplexes formed by the syn and anti conformers of **3** and **4** have different values of $\Phi_{add}$ and that solvent-induced changes in ground state conformer populations influence $\Phi_{add}$.

## Acknowledgements

Financial support for this project was provided by the National Science Foundation. We thank J.-S. Yang for some of the 2-vinylnaphthalene data, M. Gahr for the subnanosecond lifetime measurements and F.G. Bordwell for the use of the electrochemical equipment.

## References

[1] U. Mazzucato and F. Momicchioli, *Chem. Rev., 91* (1991) 1679.
[2] J. Saltiel, D.F. Sears, Jr., J.-O. Choi, Y.-P. Sun and D.W. Eaker, *J. Phys. Chem., 98* (1994) 35. J. Saltiel, N. Tarkalanov and D.F. Sears, Jr., *J. Am. Chem. Soc., 117* (1995) 5586.
[3] G. Bartocci, F. Masetti, U. Mazzucato and G. Marconi, *J. Chem. Soc., Faraday Trans. 2, 80* (1984) 1093.
[4] F.D. Lewis, B.A. Yoon, T. Arai, T. Iwasaki and K. Tokumaru, *J. Am. Chem. Soc., 117* (1995) 3029.
[5] J. Saltiel, J.-O. Choi, D.F. Sears, Jr., D.W. Eaker, K.E. O'Shea and I. Garcia, *J. Am. Chem.Soc., 118* (1996) 7478.
[6] A.S. Cherkasov, *Dokl. Acad. Sci. USSR, 146* (1962) 852.
[7] K. Gustav and H. Schreiber, *Z. Chem., 24* (1984) 409.
[8] J.F. Pfanstiel and D.W. Pratt, *J. Phys. Chem., 99* (1995) 7258.
[9] H. Tanaka, K. Honda and N. Suzuki, *J. Chem. Soc., Chem Commun.*, (1977) 506. H. Tanaka, S. Takamuku and H. Sakurai, *Bull. Chem. Soc. Jpn., 52* (1979) 801.

[10] I.B. Berlman, *Fluorescence Spectra of Aromatic Molecules*, Academic Press, New York, 1971.
[11] D.R. James, A. Siemiarczuk and W. Ware, *Rev. Sci. Instrum., 63* (1992) 1710.
[12] F.D. Lewis and D.E. Johnson, *J. Photochem., 7* (1977) 421.
[13] A.D. Bacon and M.C. Zerner, *Theor. Chim. Acta, 53* (1970) 21. M.C. Zerner, G.H. Loew, R.R. Kirchner and U.T. Mueller-Westerhoff, *J. Am. Chem. Soc., 102* (1980) 589. J. Ridley and M. Zerner, *Theor. Chim. Acta, 32* (1973) 111. W.P. Anderson, W.D. Edwards and M.C. Zerner, *Inorg. Chem., 25* (1986) 2728.
[14] F.D. Lewis, G.D. Salvi, D.R. Kanis and M.A. Ratner, *Inorg. Chem., 32* (1993) 1251.
[15] CHEM 3D PLUS, Cambridge Scientific Computing, Inc., Cambridge, MA, 1990.
[16] S. Sugasawa and H. Matsuo, *Chem. Pharm. Bull., 8* (1960) 819.
[17] V.M. Rodionov and B.I. Kurtev, *Izv. Akad. Nauk SSSR, Otd. Khim. Nauk.*, (1952) 113. S. Ono and M. Uehara, *Bull. Univ. Osaka Prefect., Ser. A, 5* (1957) 139.
[18] K.L. Facchine, S.W. Staley, P.C.M. van Zijl, P.K. Mishra and A.A. Bothner-By, *J. Am. Chem. Soc., 110* (1988) 4900.
[19] M.E. Kronenberg and E. Havinga, *Recueil, 84* (1965) 17.
[20] F.D. Lewis, J.E. Elbert, A.L. Upthagrove and P.D. Hale, *J. Org. Chem., 56* (1991) 553.
[21] R.J. Platt, *Chem. Phys., 18* (1950) 1168.
[22] S.M. de B. Costa, A.L. Maçanita and M.J. Prieto, *J. Photochem., 11* (1979) 109.
[23] G. Bartocci, F. Masetti, U. Mazzucato, A. Spalletti and M.C. Bruni, *J. Chem. Soc., Faraday Trans. 2, 82* (1986) 775.
[24] F.D. Lewis, S.L. Quillen, J.E. Elbert, S. Schneider and P. Geiselhart, *J. Photochem. Photobiol. A: Chem., 47* (1989) 173. F.D. Lewis and B.A. Yoon, *J. Photochem. Photobiol. A: Chem., 87* (1995) 193.
[25] F.D. Lewis and B.A. Yoon, *J. Org. Chem., 59* (1994) 2537.
[26] F.D. Lewis, D.M. Bassani, R.A. Caldwell and D.J. Unett, *J. Am. Chem. Soc., 116* (1994) 10 477.
[27] T. Wismontski-Knittel, I. Sofer and P.K. Das, *J. Phys. Chem., 87* (1983) 1745.
[28] F.D. Lewis and T.-I. Ho, *J. Am. Chem. Soc., 99* (1977) 7991. F.D. Lewis, *Acc. Chem. Res., 12* (1979) 152.
[29] F.D. Lewis and D.M. Bassani, *J. Photochem. Photobiol. A: Chem., 81* (1994) 13.
[30] A. Weller, *Z. Phys. Chem. (Wiesbaden), 133* (1982) 93.
[31] S. Takamuku, T. Kuroda and H. Sakurai, *Chem. Lett.*, (1982) 377.
[32] Y. Shirota, personal communication, 1984.